

A Deep Reinforcement Learning-Based Controller for Magnetorheological-Damped Vehicle Suspension

AmirReza BabaAhmadi¹, Masoud ShariatPanahi², Moosa Ayati³

^{1,2,3} School of Mechanical Engineering, College of Engineering, University of Tehran, Tehran, Iran

Abstract

This paper proposes a novel approach to controller design for an MR-damped vehicle suspension system. This approach is predicated on the premise that the optimal control strategy can be “learned” through real-world or simulated experiments utilizing a reinforcement learning algorithm with continuous states/actions. The sensor data is fed into a Twin Delayed Deep Deterministic Policy Gradient (TD3) algorithm, which generates the actuation voltage required for the MR damper. The resulting suspension working space (displacement), sprung mass acceleration, and dynamic tire load are calculated using a quarter vehicle model incorporating the modified Bouc-Wen MR damper model. Deep RL’s reward function is based on sprung mass acceleration. The proposed approach outperforms traditional suspension control strategies regarding ride comfort and stability, as demonstrated by multiple simulated experiments.

Keywords: Magnetorheological-damped suspension, ride comfort, deep reinforcement learning

1. Introduction

As one of the most critical components of the vehicle, the suspension system significantly improves ride comfort and road holding, preventing damage and reducing passenger fatigue. Suspension systems are classified as passive, active, or semi-active. Due to the fixed and unchanging nature of passive suspension parameters, passive suspension cannot guarantee ride comfort and stability when the environment or suspension parameters vary. Thus, active and semi-active suspension systems with tunable parameters can compensate for the limitations mentioned above of passive suspension systems. The uncertainty inherent in the suspension system’s road roughness and parameter variation in real applications is unavoidable.

MR fluid dampers are adaptive controllable devices that have garnered significant interest due to their simplicity, low power consumption, and high capacity force, among other characteristics. MR dampers have found widespread application in a variety of industries, including the automotive industry [1][2], civil structures [3][4], and railway vehicles [5]. MR dampers are semi-active devices because we can simply apply voltage to their coils rather than using a mechanism for the damper to produce damping force directly. As a result, two distinct controller types are required to regulate semi-active suspensions. First, the system controller calculates the required

damping force to ensure ride comfort and road holding simultaneously. The system controller inputs are derived from the suspension system's state feedback. Second, the damper controller determines the voltage that should be applied to the MR-damper for its current force to track the force specified by the system controller.

Numerous control techniques for semi-active suspension systems have been developed. H^∞ control [6], [7], [8], skyhook control [9], [10], [11], adaptive control based on neural networks [12], robust control [13], LQG control [14], [15], and optimal PID control [16][17] are some of the studies that have been conducted to develop an efficient controlling system for improving ride comfort and stability. According to previous research, PID controllers have a simple structure but are ineffective in semi-active suspension systems with uncertain parameters. Skyhook suspension control is a classic semi-active suspension control method described in [18]. It features simple structures, straightforward implementation, and acceptable performance. On the other hand, the time delay significantly affects suspension performance, resulting in instability and wheel jump. The authors of [19] designed an optimal LQG controller, but the control parameters were calculated by ignoring uncertain factors in the system modeling.

When the system's parameters change sufficiently, the system becomes unstable. The authors of [20] aimed to address the issue of the blind design of the fuzzy controller, where this was, in fact, a PID controller, and a PID was designed using rule description. Indeed, developing a proper fuzzy control system necessitates extensive knowledge of the system. The sliding mode controller in [21] shows good performance and robust behavior. On the other hand, chattering is a fatal flaw in sliding mode control. Chattering may result in instability due to the controlled system's activated high-frequency modes. Although the adaptive controller in [12] improves ride comfort, it performs poorly in road holding. Reference [22] proposed a fast model prediction controller (FMPC). The authors of [23] proposed a robust model prediction controller (RMPC).

Both of the aforementioned predictive controllers utilized road models in advance of designing controllers. The primary goal of developing a predictive controller is to provide highly accurate information from the system, which is impossible when driving on various roads with high uncertainty. In [24], it is demonstrated that neural-networked-based controllers can solve complex and nonlinear problems. However, like many other supervised learning algorithms, neural networks require a large number of labeled samples. When developing the control effort, only the current state is considered; future states are not considered. These critical issues impose constraints on the use of neural network controllers. Reference [25] proposes a novel nonlinear adaptive smart controller based on the classification of road profiles. The primary disadvantage of this method is that a new classifier must be constructed when the control strategy changes.

With the advent of Deep Learning (DL) techniques that overcome several of the significant limitations of classical machine learning algorithms, some researchers attempted to apply DL algorithms to the suspension control problem. The authors of [26] propose a DDPG-based algorithm for a particular type of suspension system. The primary drawback of this algorithm is its inability to locate the globally optimal solution to a problem.

Two types of controllers are required to control a semi-active suspension system. A system controller analyzes the system's feedback samples and predicts the desired damping force. The damper controller receives the system controller's predicted force and suspension system displacement; it then predicts the applied voltage exerted on damper coils.

The paper proposes an improved DRL controller that combines a system controller and a damper controller to provide the best ride comfort and stability possible. Notably, MR-based suspension systems operate in two modes: open-loop mode (without the use of a controller) operates with a constant damping coefficient, similar to passive suspension systems. Both the system and damper controllers work in a closed-loop system to adjust the damping force in response to road conditions by tuning the required damper's voltage input.

2. MR-damped suspension model

A simplified quarter-vehicle model with a semi-active suspension is shown in Fig. 1, where m_b represents the vehicle's body mass, m_w represents the wheel mass, and x_b and x_w denote body displacement and wheel displacement, respectively. The road profile is denoted by x_r . The spring stiffness of the suspension system is k_s , and the tire spring stiffness is denoted by k_t . We exclude tire damping from this study due to its negligible value. Table 1 contains parameters taken from [27]. Newton's second law is applied to the quarter-model of the vehicle to derive the following equations:

$$m_b \ddot{x}_b + K_s(x_b - x_w) + f = 0 \quad (1)$$

$$m_w \ddot{x}_w - K_s(x_b - x_w) + K_t(x_w - x_r) - f = 0 \quad (2)$$

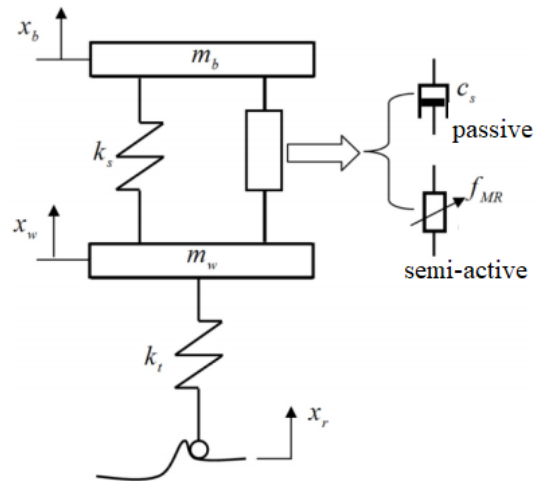


Fig. 1. A quarter-car model with two operational modes for a semi-active suspension system (passive and semi-active)

Where the following equation gives the damping force generated by the MR device:

$$f = \begin{cases} C_s(\dot{X}_b - \dot{X}_w) & \text{for passive suspension} \\ f_{MR} & \text{for semi - active suspension} \end{cases} \quad (3)$$

C_s is a coefficient describing the MR passive suspension mode of operation in an MR-damper.

The state-space representation of the semi-active suspension system is prepared as follows [17]:

$$\dot{w} = Aw + Bf_{MR} + Dx_r \quad (4)$$

$$w = [x_b \quad x_w \quad \dot{x}_b \quad \dot{x}_w]^T \quad (5)$$

$$A = \begin{bmatrix} 0 & 0 & 1 & 0 \\ 0 & 0 & 0 & 1 \\ -\frac{K_s}{m_s} & \frac{K_s}{m_s} & 0 & 0 \\ \frac{K_s}{m_w} & -\frac{K_s+K_t}{m_w} & 0 & 0 \end{bmatrix} \quad (6)$$

$$B = \begin{bmatrix} 0 & 0 & -\frac{1}{m_s} & \frac{1}{m_w} \end{bmatrix}^T \quad (7)$$

$$D = \begin{bmatrix} 0 & 0 & 0 & \frac{K_t}{m_w} \end{bmatrix}^T \quad (8)$$

Table 1. Semi-active suspension parameters [27]

Parameter	Symbol	Value (Unit)
Vehicle body mass	m_b	375(kg)
Vehicle wheel mass	m_w	29.5 (kg)
Suspension stiffness	k_s	20.58 (KN/m)
Damping coefficient	C_s	772 (Ns/m)
Tire stiffness	k_t	200 (KN/m)

Magnetorheological damper force is denoted by f_{mr} depending on the time series of the external voltage to its magnetic coil V and relative displacement $x=x_b-x_w$, which is known as suspension working space (SWS). f_{mr} is computed from Eq. 9, the modified Bouc-Wen model, derived from [28] and incorporated into the suspension system shown in Fig. 1.

$$F(t) = c_1\dot{y} + k_1(x - x_0) \quad (9)$$

$$\dot{z} = -\gamma|\dot{x} - \dot{y}||z||z|^{n-1} - \beta(\dot{x} - \dot{y})|z|^n + A(\dot{x} - \dot{y}) \quad (10)$$

$$\dot{y} = \frac{1}{c_1+c_0}\{\alpha z + k_0(x - y) + c_0\dot{x}\} \quad (11)$$

$$\alpha = a_a + a_b u \quad (12)$$

$$c_1 = c_{1a} + c_{1b} u \quad (13)$$

$$c_0 = c_{0a} + c_{0b} u \quad (14)$$

$$\dot{u} = -\eta(u - v) \quad (15)$$

The internal movement of the MR-damper is denoted as y . u is the output signal from a first-order filter, and z is a parameter that guarantees the hysteretic behavior of MR fluid. Accumulator stiffness is denoted by k_t . C_0 and C_1 represent viscous damping at high and low velocity for the

MR-damper, respectively. The stiffness regulator at high damper velocity is denoted by K_0 . MR damper accumulator simulation is performed via X_0 . The scale and shape of the hysteresis behavior of the MR-damper parameters for the simulation are γ , β , δ and η , respectively.

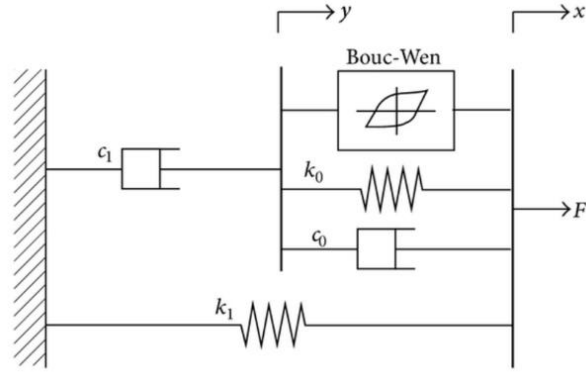


Fig. 2. Modified Bouc-Wen model for the MR-damper

Parameters for the modified Bouc-Wen MR-damper model are presented in Table 2 (adapted from [28].)

Table 2. Modified Bouc-Wen parameters for the MR-damper [28]

Parameter	Value	Parameter	Value
c_{0a}	$784 \text{ Nsm}^{(-1)}$	α_b	$38430 \text{ NsV}^{(-1)}\text{m}^{(-1)}$
c_{0b}	$1803 \text{ NsV}^{(-1)}\text{m}^{(-1)}$	β	2059020 m^{-2}
c_{1a}	$14649 \text{ Nsm}^{(-1)}$	γ	136320 m^{-2}
c_{1b}	$34622 \text{ NsV}^{(-1)}\text{m}^{(-1)}$	η	190 s^{-1}
k_1	$840 \text{ Nm}^{(-1)}$	A	58
k_0	$3610 \text{ Nm}^{(-1)}$	n	2
α_a	$12441 \text{ Nm}^{(-1)}$	x_0	0.245

2.1. Control Strategy based on DRL-TD3

As previously stated, the Twin Delayed Deep Deterministic Policy Gradient (TD3) was used as the universal controller for the MR-damped suspension system. TD3 is identical to DDPG but incorporates three additional features to address DDPG issues.

- **Clipped double Q learning:** In TD3, we compute the Q value using two critic networks and the target value using two target networks. We used only one critic and one target network in DDPG. In TD3, we use two target critic networks to compute two target Q

values. Then, when computing the loss function, we choose the smaller of the two. This will ensure that we do not overestimate the target Q value.

- **Delayed policy update:** Unlike DDPG, we added a delay to the actor-network parameter update in TD3. While the parameters of the critic networks are updated at each step of the episode, the actor-network (policy network) is delayed and updated after every two steps.
- **Target policy smoothing:** In DDPG, the algorithm generates distinct target values for identical actions. As a result, the target's variance would be high. Thus, we reduce variance by adding noise to the target action.

This section provides additional information about Twin Delayed Deep Deterministic Policy Gradients (TD3). In TD3, we employ six artificial neural networks, four of which are critic networks and two of which are two-actor networks.

- The main critic neural network parameters are denoted by θ_1 and θ_2
- The two target critic neural network parameters are represented by θ_1' and θ_2'
- The main actor-network parameter is denoted by ϕ
- The target actor-network parameter is denoted by ϕ'

Initially, we must initialize the two main critic network parameters, θ_1 and θ_2 , and the main critic network parameter ϕ with random values. Since the target network parameter is only a copy of the main network parameter, the two target critic network parameter θ_1' and θ_2' by copying θ_1 and θ_2 , are simply initialized, respectively. Similarly, we initialize the target actor parameter ϕ' , by just copying the main actor-network parameter ϕ . Also, the replay buffer is initialized too. Now, we select action a using the actor-network: $a = \mu_\phi(s)$. Rather than selecting the action directly, some noise ϵ is added to ensure exploration when $\epsilon \sim N(0, \sigma)$. Accordingly, the output action is expressed as follows: $a = \mu_\phi(s) + \epsilon$ (16).

Then, after performing action a , we move to the next state s' and obtain reward r . This transition information is stored in the replay buffer. During the next step, we randomly sample a minibatch of K transition (s, a, r, s') from the replay buffer. The K transition will be used for updating both the critic and actor network.

The loss function of the critic network is expressed as follows:

$$J(\theta_j) = \frac{1}{k} \sum (y_i - Q_{\theta_j}(s_i, a_i))^2 \quad \text{for } j = 1, 2 \quad (17)$$

In the preceding equation, the following applies:

The action a_i is the action produced by the actor-network as follows:

$$a_i = \mu_\phi(s) \quad (18)$$

y_i is the target value of the critic, that is

$$y_i = r_i + \gamma \min_{j=1,2} Q_{\theta_j}(s', \tilde{a}) \quad (19)$$

, and the action \tilde{a} is the action produced by the target critic network:

$$\tilde{a} = \mu_{\phi'}(s'_i) + \epsilon \text{ where } \epsilon \sim (N(0, \sigma), -c, +c) \quad (20)$$

After computing the loss of the critic network, the gradients $\nabla_{\theta_j} J(\theta_j)$ is computed, and then the critic network parameters will be updated using the gradient descent method.

$$\theta_j = \theta_j - \alpha \nabla_{\theta_j} J(\theta_j) \text{ for } j=1,2 \quad (21)$$

Now, the actor network must be updated. The objective function of the actor-network is as follows:

$$J(\phi) = \frac{1}{k} \sum_i Q_{\theta_i}(s_i, a) \quad (22)$$

It must be noted that in Eq. 22, we only use state (s_i) from the sampled K transitions (s, a, r, s') . The action a is selected by the actor-network.

$$a_i = \mu_\phi(s) \quad (23)$$

In order to maximize the objective function, the gradient of the objective function $\nabla_\phi J(\phi)$ is computed, and the parameters of the network are updated using the gradient ascent:

$$\phi = \phi + \alpha \nabla_\phi J(\phi) \quad (24)$$

We delay the update rather than updating the actor-parameters networks at each time step of the episode. If the time step of the episode is denoted by t and d denotes the number of time steps which we want to delay the update, it can be described as follows:

1- If $t \bmod d=0$, then:

1. Compute the gradient of the objective function $\nabla_{\phi} J(\phi)$

2. Update the actor-network parameter using the gradient ascent method (24).

Finally, the parameters of the target critic network θ_1' and θ_2' and the parameters of the target actor-network ϕ' will be updated via soft replacement:

$$\begin{cases} \theta_j' = \tau\theta_j + (1 - \tau)\theta_j' & \text{for } j = 1,2 \\ \phi' = \tau\phi + (1 - \tau)\phi' \end{cases} \quad (25)$$

There is a small change in updating the parameters of the target networks. As with the actor-network parameter, we delay updating it for d steps; similarly, we update the target network parameters for every d step; in this case, we can say:

1- If $t \bmod d=0$, then:

1. Compute the gradient of the objective function $\nabla_{\phi} J(\phi)$ and update the actor-network parameter using gradient ascent.

$$\phi = \phi + \alpha \nabla_{\phi} J(\phi) \quad (26)$$

2. Update the target critic network parameter and target actor-network parameter as

$$\theta_j' = \tau\theta_j + (1 - \tau)\theta_j' \quad \text{for } j = 1,2 \quad (27)$$

and

$$\phi' = \tau\phi + (1 - \tau)\phi' \quad (28)$$

, respectively.

The previous steps for several episodes must be repeated to improve the policy. The following pseudocode is prepared to understand better how TD3 works:

Twin Delayed Deep Deterministic Policy Gradient Algorithm:

```

1 Initialize critic networks  $Q_{\theta_1}, Q_{\theta_2}$ , and actor network  $\pi_\phi$ 
   with random parameters  $\theta_1, \theta_2, \phi$ 
2 Initialize target networks  $\theta'_1 \leftarrow \theta_1, \theta'_2 \leftarrow \theta_2, \phi' \leftarrow \phi$ 
   Initialize replay buffer  $\mathcal{B}$ 
   for  $t = 1$  to  $T$  do
3   Select action with exploration noise  $a \sim \pi_\phi(s) + \epsilon$ ,
      $\epsilon \sim \mathcal{N}(0, \sigma)$  and observe reward  $r$  and new state  $s'$ 
4   Store transition tuple  $(s, a, r, s')$  in  $\mathcal{B}$ 

5   Sample mini-batch of  $N$  transitions  $(s, a, r, s')$  from  $\mathcal{B}$ 
      $\tilde{a} \leftarrow \pi_{\phi'}(s') + \epsilon$ ,  $\epsilon \sim \text{clip}(\mathcal{N}(0, \tilde{\sigma}), -c, c)$ 
      $y \leftarrow r + \gamma \min_{i=1,2} Q_{\theta'_i}(s', \tilde{a})$ 
     Update critics  $\theta_i \leftarrow \text{argmin}_{\theta_i} N^{-1} \sum (y - Q_{\theta_i}(s, a))^2$ 
7   if  $t \bmod d$  then
     Update  $\phi$  by the deterministic policy gradient:
      $\nabla_\phi J(\phi) = N^{-1} \sum \nabla_a Q_{\theta_1}(s, a)|_{a=\pi_\phi(s)} \nabla_\phi \pi_\phi(s)$ 
8   Update target networks:
      $\theta'_i \leftarrow \tau \theta_i + (1 - \tau) \theta'_i$ 
      $\phi' \leftarrow \tau \phi + (1 - \tau) \phi'$ 
   end if
   end for

```

Fig. 3. TD3 Algorithm pseudocode

2.2. TD3 application in closed-loop vibration control for a semi-active suspension system

The main inputs for vehicle dynamics are road disturbance profile and damping force produced by the MR device. The outputs are body (sprung mass) acceleration and suspension working space (SWS). The RL-Agent inputs for implementing a controller for a one-quarter suspension system are body acceleration, denoted by q , and a reward function, which is as follows:

$$r = \begin{cases} 0 & \text{if } q = q_{goal} = 0 \\ -kq^2 & \text{if } q \neq 0 \end{cases} \quad (29)$$

Where k is a hyperparameter that specifies the intensity coefficient for agent punishment, the agent punishments experienced in the replay buffer are also exerted in the RL-agent. The damper's input voltage must be applied to the coil via the RL-agent output (action). TD3 analyzes its performance by measuring body acceleration and fine-tuning its action to road profile disturbances. The

surrounding environment consists of a vehicle suspension system equipped with an MR-damper and a road profile. The agent is a neural network that constructs the controller part. The hyperparameters listed in Table 3 pertain to TD3 agents used in closed-loop suspension control. Figures 5 and 6 detail the neural networks used in the TD3 algorithm.

The hidden size is 400 and 300 neurons in each layer for the actor and critic network, respectively. The optimization method is Adam for both actor and critic networks. The discount factor γ is 0.8. The input voltage varies from 0 to 3 V, and the damping force varies from -1.5 to 1.5 KN.

Table 3. Neural Networks Parameters in TD3

Network	Learning Rate	Optimizer	Delay for update
Actor	0.002	Adam	2
Critic	0.002	Adam	1
Actor Target	0.006	-	2
Critic Target	0.006	-	2

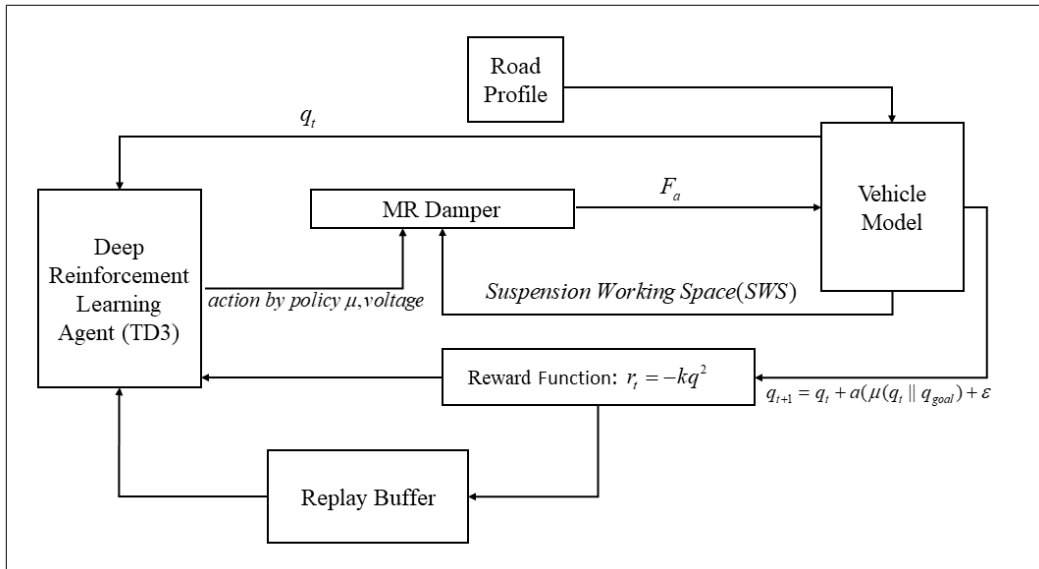


Fig. 4. Closed-loop semi-active suspension system block diagram with DRL Agent

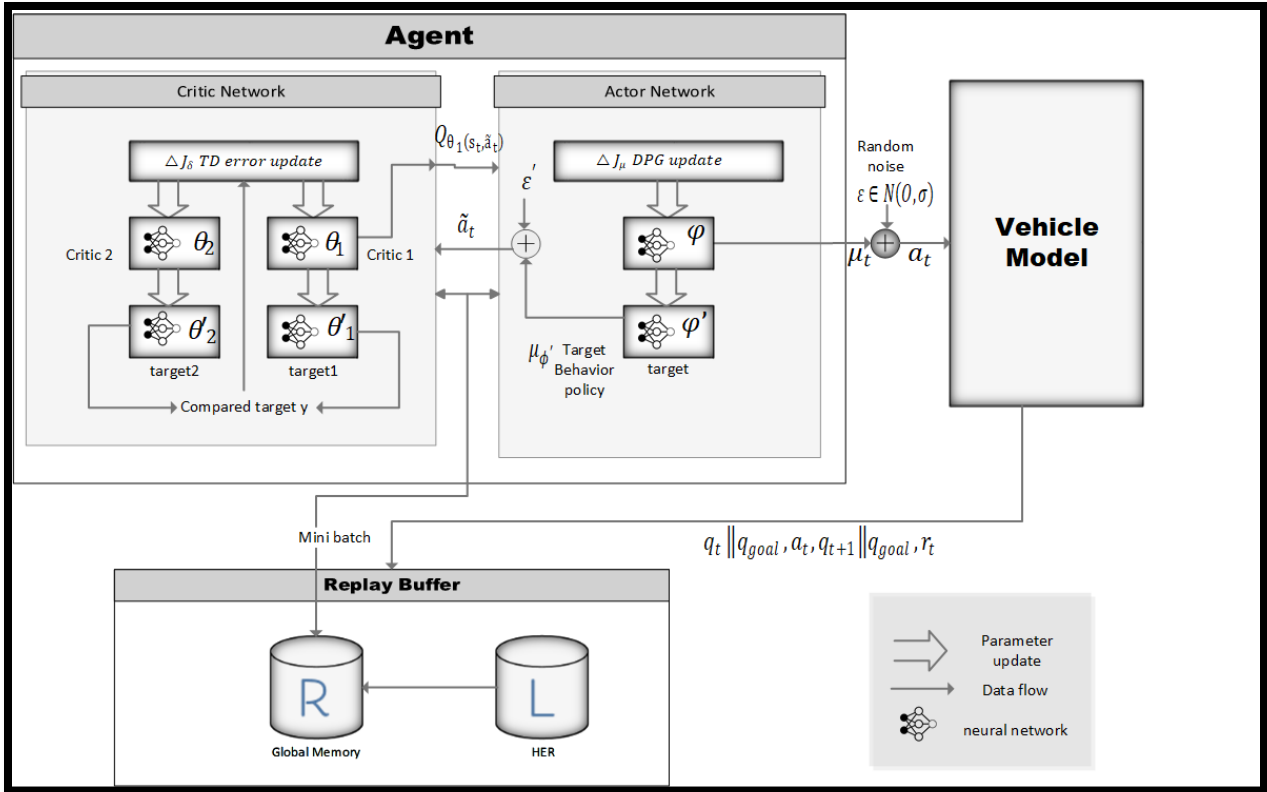


Fig. 5. Actor-critic architecture in TD3 Agent

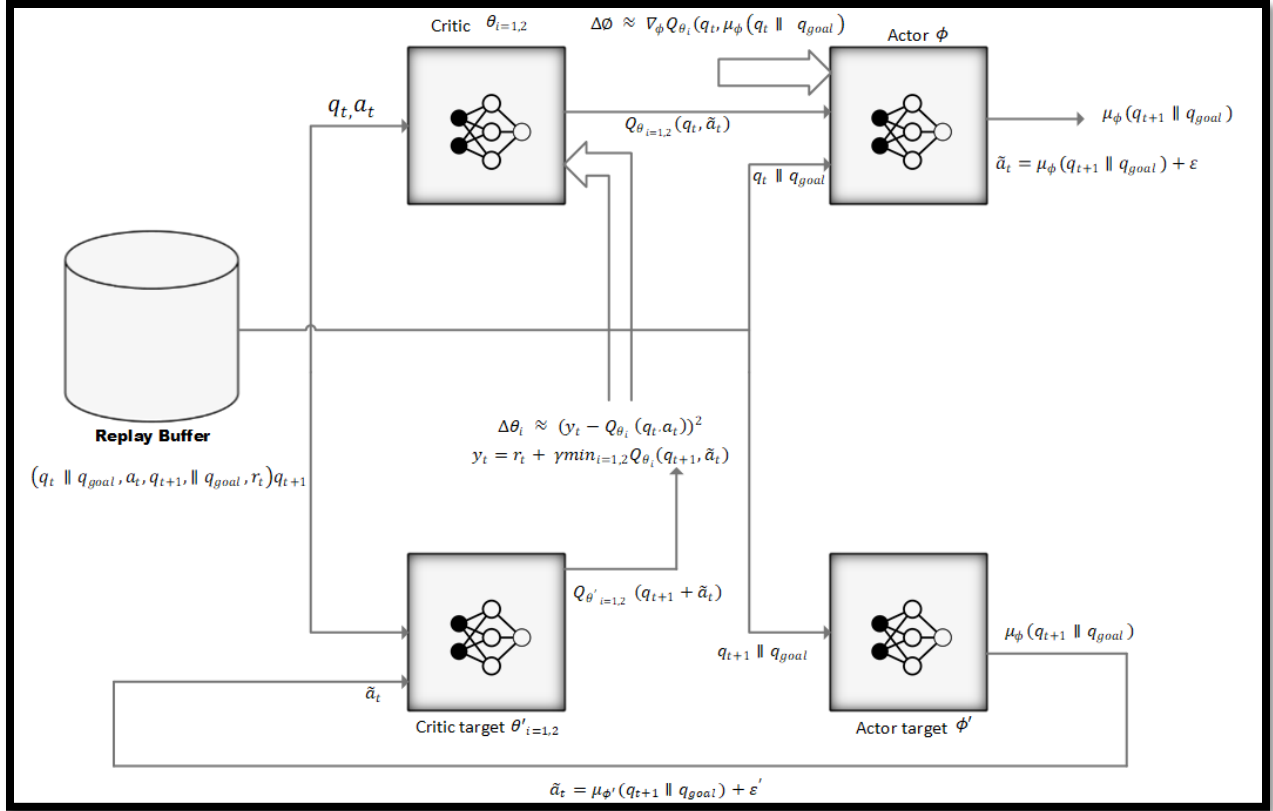


Fig. 6. The details of actor-critic networks in semi-active suspension control

3. Results and Discussion

Vertical body acceleration (BA), Dynamic Tire Load (DTL), and Suspension Working space are three primary performance criteria used in the suspension design of a vehicle to improve ride comfort and road holding, preventing the suspension system from bottoming out excessively. To achieve the objectives mentioned above, we should reduce BA or SWS to improve ride comfort and DTL to improve road holding and minimize suspension space distance. The BA has been chosen as the objective function in this article.

Two types of controllers for semi-active suspension are investigated in this section: the RL-based TD3 and the PID controller; their gains are tuned using the Particle Swarm Optimization (PSO) algorithm from [17], as well as an uncontrolled system (MR-Passive) with no applied voltage to the damper's coil.

A particular type of bump-road excitation was chosen due to its resemblance to actual road profiles. Additionally, the bump-road profile demonstrates the characteristics of transient response. The road-bump profile has been proposed in [27] as:

$$X_r = \begin{cases} a \{1 - \cos(\omega_r(t - 0.5))\}, & \text{for } 0.5 \leq t \leq 0.5 + \frac{d_b}{V_c} \\ 0, & \text{otherwise} \end{cases} \quad (1)$$

Where a denotes half of the bump amplitude, $\omega_r = 2\pi \frac{V_c}{d_b}$, d_b is the bump width, and V_c denotes the vehicle velocity. In this research, $a = 0.035m$, $d_b = 0.8m$, $V_c = 0.856 \frac{m}{s}$, derived from [27].

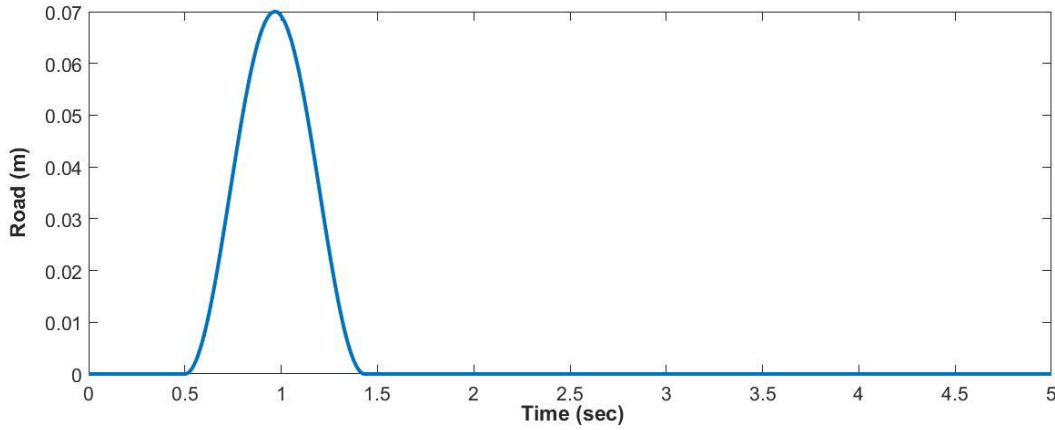


Fig. 7. Road-bump profile

Table 4 compares the results from the TD3 controller to an uncontrolled system (applied zero voltage), and Table 5 compares the results from the PSO PID controller to the TD3.

The results demonstrate unequivocally that the DRL-based controller (TD3) algorithm outperforms PSO-tuned PID. TD3 is excellent at dissipating vibrations caused by bump excitation. Additionally, it reduces settling time and enhances road holding and ride comfort.

DRL TD3 significantly reduces body acceleration, suspension working space, and Dynamic Tire Load compared to an uncontrolled suspension system by 35.8%, 68.5%, and 33.6%, respectively. Simultaneously, PSO-PID reduces those criteria by 32.2%, 50%, and 12.4%, respectively, compared to MR passive (uncontrolled suspension).

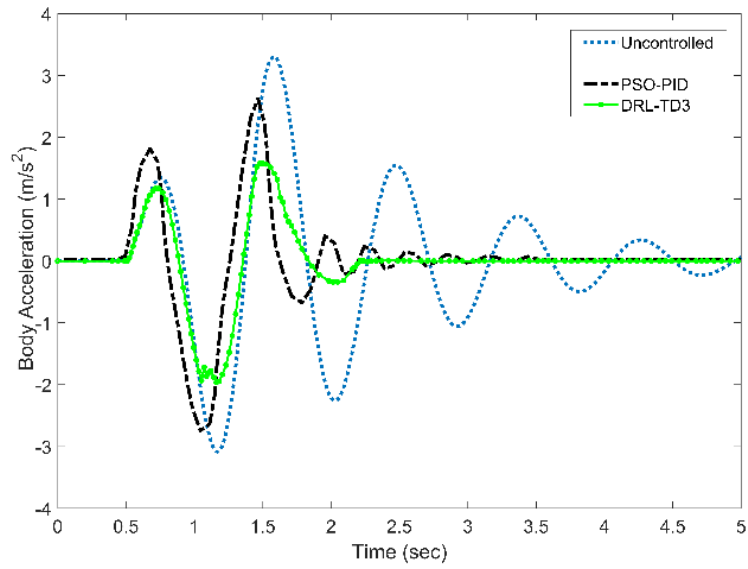


Fig. 7. Body Acceleration (BA)

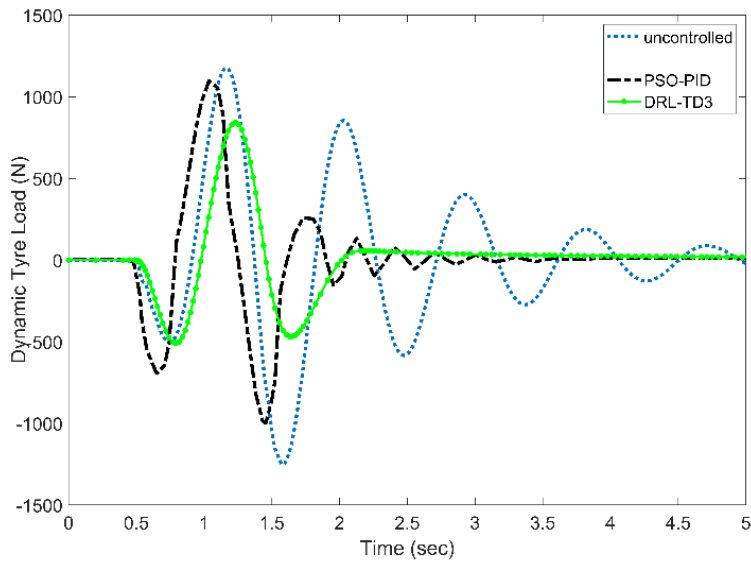


Fig. 8. Dynamic Tyre Load (DTL)

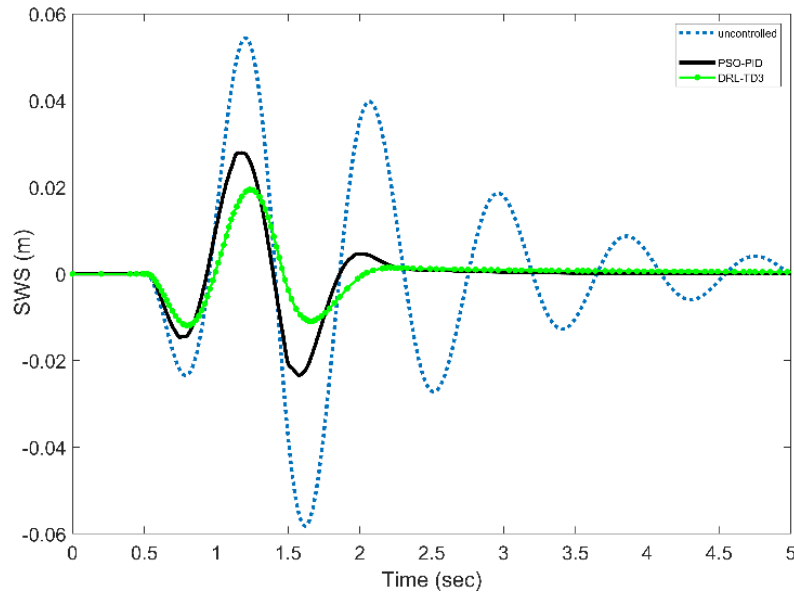


Fig. 9. Suspension Working Space (SWS)

Table 4. RMS Values for the suspension system criteria with TD3 algorithm and Uncontrolled Suspension System

RMS-values	Body Acceleration(m/s^2)	Suspension Working Space(m)	Dynamic Tire Load (N)
<i>DRL-TD3</i>	0.97	0.0084	381.32
<i>Uncontrolled</i>	1.5179	0.0267	537.7

Table 5. Comparison of DRL-TD3 with PSO-PID

Controller Type	Body Acceleration(m/s^2)	Suspension Working Space(m)	Dynamic Tire Load (N)
<i>DRL-TD3</i>	35.8 %	68.53 %	33.6%
<i>PSO-PID</i>	22.4%	46.1%	11.9%
<i>Improvement</i>	13.4%	22.43%	21.7%

4. Conclusion

The paper proposes the DRL-based TD3 algorithm for vibration mitigation in a semi-active suspension system equipped with an MR damper. Three major criteria, BA, SWS, and DTL, were considered and investigated when evaluating the proposed controller. Instead of using two distinct controllers for damper control and force estimation, a single universal controller based on real-time learning was used. The time-domain results were analyzed, and the effectiveness of the

DRL-based controller was compared to the optimal PSO-PID controller. Finally, the results demonstrate that the TD3 algorithm outperforms the PSO-tuned PID controller.

Declaration of competing interest

The authors declare that they have no known competing financial interests or personal relationships that could have appeared to influence the work reported in this paper.

References

- [1] A. H. F. Lam and W. H. Liao, "Semi-active control of automotive suspension systems with magnetorheological dampers," *Int. J. Veh. Des.*, vol. 33, no. 1–3, pp. 50–75, 2003, doi: 10.1504/ijvd.2003.003652.
- [2] M. A. Karkoub and M. Zribi, "Active/semi-active suspension control using magnetorheological actuators," *Int. J. Syst. Sci.*, vol. 37, no. 1, pp. 35–44, Jan. 2006, doi: 10.1080/00207720500436344.
- [3] S. J. Dyke, B. F. Spencer, M. K. Sain, and J. D. Carlson, "Modeling and control of magnetorheological dampers for seismic response reduction," *Smart Mater. Struct.*, vol. 5, no. 5, pp. 565–575, Oct. 1996, doi: 10.1088/0964-1726/5/5/006.
- [4] K. A. Bani-Hani and M. A. Sheban, "Semi-active neuro-control for base-isolation system using magnetorheological (MR) dampers," *Earthq. Eng. Struct. Dyn.*, vol. 35, no. 9, pp. 1119–1144, Jul. 2006, doi: 10.1002/eqe.574.
- [5] W. H. Liao and D. H. Wang, "Semiactive Vibration Control of Train Suspension Systems via Magnetorheological Dampers," *J. Intell. Mater. Syst. Struct.*, vol. 14, no. 3, pp. 161–172, Mar. 2003, doi: 10.1177/1045389X03014003004.
- [6] H. Du, K. Yim Sze, and J. Lam, "Semi-active H_∞ control of vehicle suspension with magnetorheological dampers," *J. Sound Vib.*, vol. 283, no. 3–5, pp. 981–996, May 2005, doi: 10.1016/j.jsv.2004.05.030.
- [7] S. B. Choi, H. S. Lee, and Y. P. Park, " H_∞ control performance of a full-vehicle suspension featuring magnetorheological dampers," *Veh. Syst. Dyn.*, vol. 38, no. 5, pp. 341–360, Nov. 2002.
- [8] S. B. Choi and K. G. Sung, "Vibration control of magnetorheological damper system subjected to parameter variations," *Int. J. Veh. Des.*, vol. 46, no. 1, pp. 94–110, 2008, doi: 10.1504/IJVD.2008.017071.
- [9] H.-S. Lee and S.-B. Choi, "Control and Response Characteristics of a Magnetorheological Fluid Damper for Passenger Vehicles," *J. Intell. Mater. Syst. Struct.*, vol. 11, no. 1, pp. 80–87, Jan. 2000, doi: 10.1106/412A-2GMA-BTUL-MALT.
- [10] M. Ahmadian and C. A. Pare, "A Quarter-Car Experimental Analysis of Alternative Semiactive Control Methods," *J. Intell. Mater. Syst. Struct.*, vol. 11, no. 8, pp. 604–612, Aug. 2000, doi: 10.1106/MR3W-5D8W-0LPL-WGUQ.
- [11] Y. Shen, M. F. Golnaraghi, and G. R. Heppler, "Semi-active Vibration Control Schemes for Suspension Systems Using Magnetorheological Dampers," *J. Vib. Control*, vol. 12, no. 1, pp. 3–24, Jan. 2006, doi: 10.1177/1077546306059853.
- [12] D. L. Guo, H. Y. Hu, and J. Q. Yi, "Neural Network Control for a Semi-Active Vehicle Suspension

- with a Magnetorheological Damper,” *J. Vib. Control*, vol. 10, no. 3, pp. 461–471, Mar. 2004, doi: 10.1177/1077546304038968.
- [13] M. Zribi and M. Karkoub, “Robust Control of a Car Suspension System Using Magnetorheological Dampers,” *J. Vib. Control*, vol. 10, no. 4, pp. 507–524, Apr. 2004, doi: 10.1177/1077546303039697.
- [14] A. Elsayaf, F. Ashida, and S. I. Sakata, “Optimum structure design of a multilayer piezo-composite disk for control of thermal stress,” *J. Therm. Stress.*, vol. 35, no. 9, pp. 805–819, Sep. 2012, doi: 10.1080/01495739.2012.689233.
- [15] H. A. Metered, “Application of Nonparametric Magnetorheological Damper Model in Vehicle Semi-active Suspension System,” *SAE Int. J. Passeng. Cars - Mech. Syst.*, vol. 5, no. 1, pp. 715–726, Apr. 2012, doi: 10.4271/2012-01-0977.
- [16] S. Gad, H. Metered, A. Bassuiny, and A. M. Abdel Ghany, “Vibration control of semi-active MR seat suspension for commercial vehicles using genetic PID controller,” in *Mechanisms and Machine Science*, 2015, vol. 23, pp. 721–732, doi: 10.1007/978-3-319-09918-7_64.
- [17] H. Metered, A. Elsayaf, T. Vampola, and Z. Sika, “Vibration Control of MR-Damped Vehicle Suspension System Using PID Controller Tuned by Particle Swarm Optimization,” *SAE Int. J. Passeng. Cars - Mech. Syst.*, vol. 8, no. 2, pp. 426–435, Jul. 2015, doi: 10.4271/2015-01-0622.
- [18] J. Yao, S. Taheri, S. Tian, Z. Zhang, and L. Shen, “A novel semi-active suspension design based on decoupling skyhook control,” *J. Vibroengineering*, vol. 16, no. 3, 2014.
- [19] Y. YU, C. ZHOU, L. ZHAO, Y. XING, ... P. S.-J. of S., and undefined 2017, “Design of LQG controller for vehicle active suspension system based on alternate iteration,” *en.cnki.com.cn*, Accessed: Apr. 18, 2021. [Online]. Available: https://en.cnki.com.cn/Article_en/CJFDTotal-SDGY201704009.htm.
- [20] D. Wang, H. W.-C. M. Engineering, and undefined 2017, “Control method of vehicle semi active suspensions based on variable universe fuzzy control,” *en.cnki.com.cn*, Accessed: Apr. 18, 2021. [Online]. Available: https://en.cnki.com.cn/Article_en/CJFDTotal-ZGJX201703019.htm.
- [21] J. L. Yao, W. K. Shi, J. Q. Zheng, and H. P. Zhou, “Development of a sliding mode controller for semi-active vehicle suspensions,” *JVC/Journal Vib. Control*, vol. 19, no. 8, pp. 1152–1160, Jun. 2013, doi: 10.1177/1077546312441045.
- [22] M. Canale, M. Milanese, and C. Novara, “Semi-active suspension control using ‘fast’ model-predictive techniques,” *IEEE Trans. Control Syst. Technol.*, vol. 14, no. 6, pp. 1034–1046, Nov. 2006, doi: 10.1109/TCST.2006.880196.
- [23] D. Wang, D. Zhao, M. Gong, and B. Yang, “Research on Robust Model Predictive Control for Electro-Hydraulic Servo Active Suspension Systems,” *IEEE Access*, vol. 6, pp. 3231–3240, Dec. 2017, doi: 10.1109/ACCESS.2017.2787663.
- [24] “Neural network control method of automotive semi-active air suspension-- 《Journal of Traffic and Transportation Engineering》 2006年04期.” https://en.cnki.com.cn/Article_en/CJFDTotal-JYGC200604014.htm (accessed Apr. 18, 2021).
- [25] Y. Qin, J. J. Rath, C. Hu, C. Sentouh, and R. Wang, “Adaptive nonlinear active suspension control based on a robust road classifier with a modified super-twisting algorithm,” *Nonlinear Dyn.*, vol. 97, no. 4, pp. 2425–2442, Sep. 2019, doi: 10.1007/s11071-019-05138-8.
- [26] L. Ming, L. Yibin, R. Xuewen, Z. Shuaishuai, and Y. Yanfang, “Semi-active suspension control based on deep reinforcement learning,” *IEEE Access*, vol. 8, pp. 9978–9986, 2020, doi:

10.1109/ACCESS.2020.2964116.

- [27] S. B. Choi, Y. T. Choi, and D. W. Park, "A sliding mode control of a full-car electrorheological suspension system via hardware in-the-loop simulation," *J. Dyn. Syst. Meas. Control. Trans. ASME*, vol. 122, no. 1, pp. 114–121, Mar. 2000, doi: 10.1115/1.482435.
- [28] C. Y. Lai and W. H. Liao, "Vibration Control of a Suspension System via a Magnetorheological Fluid Damper," *J. Vib. Control*, vol. 8, no. 4, pp. 527–547, Apr. 2002, doi: 10.1177/107754602023712.